CMS Physics Analysis Summary

Contact: cms-pag-conveners-exotica@cern.ch 2013/05/02

Search for Jet Extinction in the Inclusive Jet p_{T} Spectrum at $\sqrt{s} = 8$ TeV

The CMS Collaboration

Abstract

A search for the extinction of QCD jet production is presented using data collected with the CMS detector corresponding to 10.7 fb^{-1} of proton-proton collisions at $\sqrt{s} = 8$ TeV. The extinction model studied in this analysis is motivated by the search for signatures of terascale gravity at the LHC and assumes the existence of string couplings in the strong-coupling limit. In this limit, the string model predicts suppression of all high transverse momentum standard model processes, including jet production, beyond a certain energy scale. A shape comparison between the measured transverse momentum spectrum of jets and the theoretical prediction is conducted. No significant deficit of events is found at high transverse momentum. A 95% CL lower limit of 3.3 TeV is set on the extinction energy scale.

1 Introduction

The scattering of high energy particles in theories of quantum gravity is fundamentally different from that expected by the local quantum field theories of the standard model (SM) [1]. The Planck scale, the threshold at which quantum gravity becomes strong, is therefore a fundamental boundary beyond which some modification to the SM is required. The Planck scale differs from the electroweak scale by some 16 orders of magnitude, creating what is commonly known as a hierarchy problem. There are many models which therefore propose a mechanism by which these two scales are related to one another, through the hypothesized existence of extra dimensions. Propagation of gravitons through these extra dimensions then explains the relative weakness of gravity compared to the strong and electroweak interactions. Depending on the model, a variety of striking signatures of new physics may be observed. As a result, models which predict strong gravity at the TeV scale (terascale gravity), have been the subject of numerous searches at the LHC [2–10].These searches are designed to look for such effects as resonant production and decay of new states like Randall–Sundrum gravitons [11], continuum enhancements to SM processes from both virtual and direct graviton production [12], and events with high transverse momentum (p_{T}) and multiple objects from the decay of high-entropy intermediate states, often referred to as microscopic black holes [1, 13, 14].

As of yet, no signal indicative of terascale gravity has been found. Nevertheless, it has been suggested that evidence of terascale gravity could also be found through more subtle effects on the jet p_{T} spectrum manifesting themselves as a deviation from the predictions of quantum chromodynamics (QCD) [1, 13, 15, 16]. While the production of either black holes or other non-perturbative quantum gravity effects can have a rapidly increasing total cross section beyond some energy scale, their decay to isolated jets or other low-multiplicity final states could be thermally suppressed, leading to a full suppression of high-p_{T} SM scattering processes (jet extinction). Because jet production is the leading SM process at high p_{T}, such effects would be noticeable there first as a jet extinction signature [16]. In this sense the search for jet extinction is complementary to searches for black holes in high-multiplicity final states. These final states arise in the asymptotic limit where black holes are expected to behave classically [14]. The extinction search explores an intermediate regime where a high-multiplicity signature may not be readily observable.

There are several models that include extinction phenomena [15, 16]. In this analysis, we consider a model with a large width Veneziano form factor modification of QCD processes with an extinction scale M equivalent to the fundamental Planck scale [16]. Beyond the scale M, the predominance of intermediate high-entropy string states will suppress high-p_{T} SM jet production. This search exploits the measurement of the differential jet production cross-section in p_{T} at the Compact Muon Solenoid (CMS) [17] experiment to search for a deformation of the jet spectrum consistent with extinction phenomena in which there are fewer high-p_{T} jets than expected from the SM. This analysis is especially sensitive to the correlations of the systematic uncertainties across bins in jet p_{T}, so a detailed evaluation of the systematic uncertainties associated with the jet-energy scale (JES) and the parton distribution functions (PDFs) is performed.

2 The CMS Detector

The central feature of the CMS detector [18] is a superconducting solenoid of 6 m internal diameter, providing a field of 3.8 T. Within the field volume are silicon pixel and strip trackers, a crystal electromagnetic calorimeter (ECAL) and a brass/scintillator hadron calorimeter (HCAL). Muons are measured in gas-ionization detectors embedded in the steel return yoke.

Extensive forward calorimetry complements the coverage provided by the barrel and endcap detectors.

CMS uses a right-handed coordinate system, with the origin at the nominal interaction point, the x axis pointing to the center of the LHC, the y axis pointing up (perpendicular to the LHC plane), and the z axis along the counter-clockwise beam direction. The polar angle θ is measured from the positive z axis and the azimuthal angle ϕ is measured in the xy plane. The pseudorapidity η is defined as $-\ln\tan\theta/2$.

The first level (L1) of the CMS trigger system is composed of customized hardware and uses information from the calorimeters and muon detectors to select the most interesting events within 4 μs. The High Level Trigger [19] (HLT) processor farm further decreases the event rate from around 100 kHz to around 300 Hz before the data is recorded for analysis.

3 Background and Signal Modeling

The SM prediction of the jet p_{T} spectrum is calculated at next-to-leading order (NLO) with the NLOJet++ program within the fastNLO framework [20–22]. The CT10 PDF set [23] is used in this calculation. The renormalization and factorization scales, μ_{R} and μ_{F} respectively, are given a value of $\hat{p}_{\mathrm{T}}$, the transverse momentum of the hard scattered parton. The NLO jet spectra do not include non-perturbative effects or any modeling of the detector response. The non-perturbative effects, which account for hadronization and multi-parton interactions (MPI), are incorporated as corrections determined from the PYTHIA 6.424 [24] Monte Carlo (MC) generator. The generator is used to simulate QCD events with and without non-perturbative effects included. The corrections are then derived from the ratio of the resulting p_{T} spectra. The fractional NP correction decreases monotonically as a function of jet-p_{T} from 3% to 1%. This process is repeated using the HERWIG [25] generator. The difference between the corrections derived from these generators is typically taken as a source of systematic uncertainty, but is found to be negligible in the phase space of this analysis. The corrected NLO jet spectra are then convolved with a function that models the CMS detector response [26]. These smeared spectra can then be compared directly to the observed spectrum. The smeared NLO jet spectrum is referred to as $d\sigma^{QCD}/dp_{\mathrm{T}NLO}$. This procedure is then repeated to produce a smeared LO jet p_{T} spectrum, labelled as $d\sigma^{QCD}/dp_{\mathrm{T}LO}$.

The effects of extinction at leading order (LO) are also modeled using the PYTHIA MC generator. The matrix elements of each color channel are modified by Veneziano-type form factors [16] that affect all $2 \to 2$ scattering amplitudes. The input parameters for these form factors are the extinction scale M and a unitless width parameter. For small values of the width parameter, these form factors are similar to those that describe string resonances [27, 28]. This is referred to as the weak-coupling limit. The regime where the width is close to one is known as the strong-coupling limit. In this limit, extinction physics rapidly overwhelms leading order SM processes as well as any resonant string production. Beyond the scale M, scattering processes are dominated by a continuum of high-entropy intermediate states that results in suppression of SM jet production (jet extinction) [16]. This search assumes a width parameter of one, the absolute strong-coupling limit of the string model. Values of the width above one represent a very different phenomenology where the form factors no longer monotonically decrease as a function of jet momentum.

The effects of extinction are predominantly found in $2 \to 2$ scattering processes. Such processes are dominated by the LO calculation at a given p_{T} scale. We approximate the signal with a LO generator. The extinction process is assumed to have a very weak effect on higher-order

interactions. A sigmoidal function provides a good functional fit of the effect of the Veneziano form factors on the LO jet p_{T} spectrum [16]. This yields the following equation for the jet-p_{T} spectrum assuming extinction at LO:

$$\frac{d\sigma^{Extinction}}{dp_{\mathrm{T}LO}} = \frac{\frac{d\sigma^{QCD}}{dp_{\mathrm{T}LO}}}{1 + exp\frac{p_{\mathrm{T}} - p_{\mathrm{T},1/2}(M)}{p_{\mathrm{T},0}(M)}} \tag{1}$$

and at NLO:

$$\frac{d\sigma^{Extinction}}{dp_{\mathrm{T}NLO}} = \frac{d\sigma^{QCD}}{dp_{\mathrm{T}NLO}} - \frac{d\sigma^{QCD}}{dp_{\mathrm{T}LO}} + \frac{\frac{d\sigma^{QCD}}{dp_{\mathrm{T}LO}}}{1 + exp\frac{p_{\mathrm{T}} - p_{\mathrm{T},1/2}(M)}{p_{\mathrm{T},0}(M)}} \tag{2}$$

Here, $p_{\mathrm{T},1/2}$ describes the p_{T} threshold at which the extinction manifests, while $p_{\mathrm{T},0}$ indicates how quickly beyond $p_{\mathrm{T},1/2}$ the LO cross-section becomes negligible. Several simulations of LO jet production are performed assuming values of M between 2 and 5 TeV in increments of 500 GeV. The jet-p_{T} spectrum is then produced at NLO for each sample using NP corrections and resolution smearing as described above. The values of $p_{\mathrm{T},1/2}(M)$ and $p_{\mathrm{T},0}(M)$ are extracted from a fit of the product of SM jet production and $F(p_{\mathrm{T}}, M)$ to the expected p_{T} distribution for different values of M. $p_{\mathrm{T},0}(M)$ is nearly independent of M and ranges between 260 and 330 GeV, while $p_{\mathrm{T},1/2}(M)$ is about half the extinction scale.

For finite values of M, the predicted jet p_{T} spectrum is suppressed above M. At very large values of M, the SM and extinction spectra become identical.

4 Event Reconstruction and Selection

A particle-flow algorithm [29] is used to reconstruct the events. Jets are formed by clustering the reconstructed particle-flow objects using the anti-k_{T} algorithm [30] with a distance parameter of 0.7. The jet momentum is the vectorial sum of all particle momenta in the jet and is found to be within 5–10% of the simulated jet momenta over the entire p_{T} spectrum and detector acceptance. Jet-energy corrections are derived from simulation and are confirmed with in situ measurements of energy balance in dijet and photon-plus-jet events. The relative jet energy resolution (JER) is approximately 4% at 1 TeV. To suppress spurious signals from detector noise [31], jets are required to satisfy stringent selection criteria [32]. Specifically, each jet must contain at least two particles, one of which is a charged hadron. Additionally, each of the jet-energy fractions carried by neutral hadrons, photons, electrons and muons must be less than 90%.

The data used in this analysis were collected from an HLT trigger path that accepted events containing at least one jet with $p_{\mathrm{T}} > 320$ GeV. An offset is applied to subtract the energy deposited in each jet due to pile-up effects, and does not impact the trigger efficiency. Events with objects originating from an interaction within an LHC beam crossing are selected by requiring the presence of at least one well-reconstructed primary vertex within 24 cm of the detector center. Additionally, the missing transverse energy, defined as the magnitude of the vector sum of the transverse momenta of reconstructed particle-flow objects, must be less than 30% of the total transverse energy deposited in the detector. All jets in each event that pass the selection criteria are binned in a commonly-used p_{T} binning shared among inclusive-jet analyses in CMS. The bins have variable width that increase with jet p_{T} and correspond to the jet p_{T} resolution [17].

We require jets to have $p_T > 592$ GeV and pseudorapidity $|\eta| < 1.5$ to ensure that the trigger is at least 99% efficient in all p_T bins used. This search is performed in 18 p_T bins between 592 and 2500 GeV.

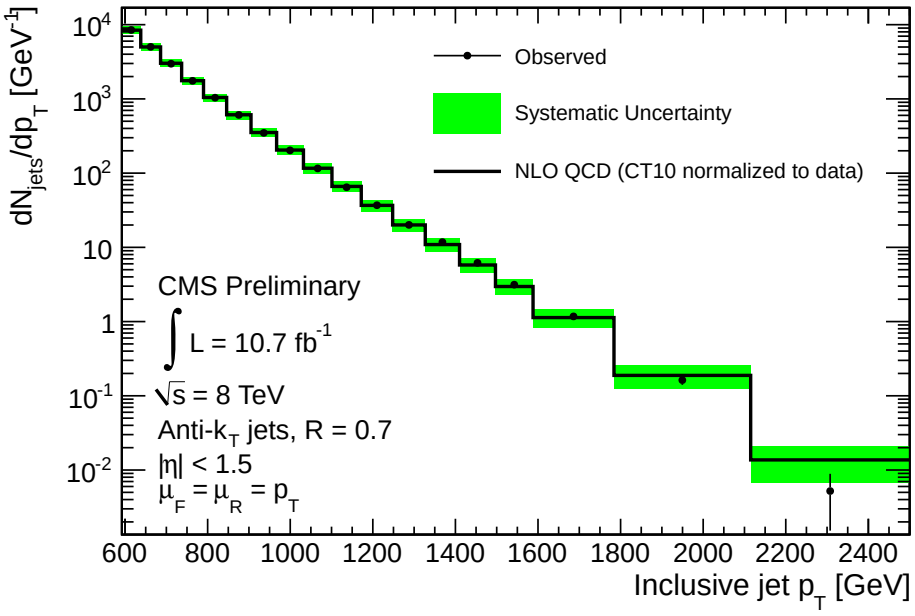

Figure 1: Inclusive jet p_T spectrum (points) for $|\eta| < 1.5$, as observed in 10.7 fb^{-1} of data. The SM NLO simulation with non-perturbative corrections, convolved with the detector response and normalized to the total observed cross-section, is shown by the solid line. The colored band shows the magnitude of all sources of systematic uncertainty added in quadrature. These sources include the JES, JER, PDFs, and luminosity. Normalization to the observed total cross-section is not performed during the likelihood comparison between data and theory. The renormalization scale (μ_R) and factorization scale (μ_F) are set to jet p_T.

A comparison between the observed inclusive jet p_T spectrum and the spectrum predicted at NLO with the CT10 PDF set is shown in figures 1 and 2. The CT10 prediction includes non-perturbative corrections and smearing by the detector response, and is normalized to the total number of jets in the data. In both figures, we show the magnitude of all sources of systematic uncertainty added in quadrature at 1σ. The total systematic uncertainty includes contributions from both theoretical and experimental sources. The theoretical uncertainty is composed of the uncertainty from the PDFs as well as uncertainty obtained by varying the renormalization and factorization scales. The experimental uncertainty is derived from the uncertainty in the JES, JER, and luminosity. Figure 2 shows the ratio of the inclusive spectrum to the SM NLO expectation and includes the predicted spectra from the extinction model for three different values of the extinction parameter M.

5 Statistical Method and Systematic Uncertainties

To distinguish between SM NLO jet production and the alternative hypothesis (jet extinction), we construct a profile-likelihood ratio test statistic [33] as a function of a signal strength parameter, $\beta \equiv M^{-2}$. Using μ to refer to the signal strength, a likelihood ratio is established as follows:

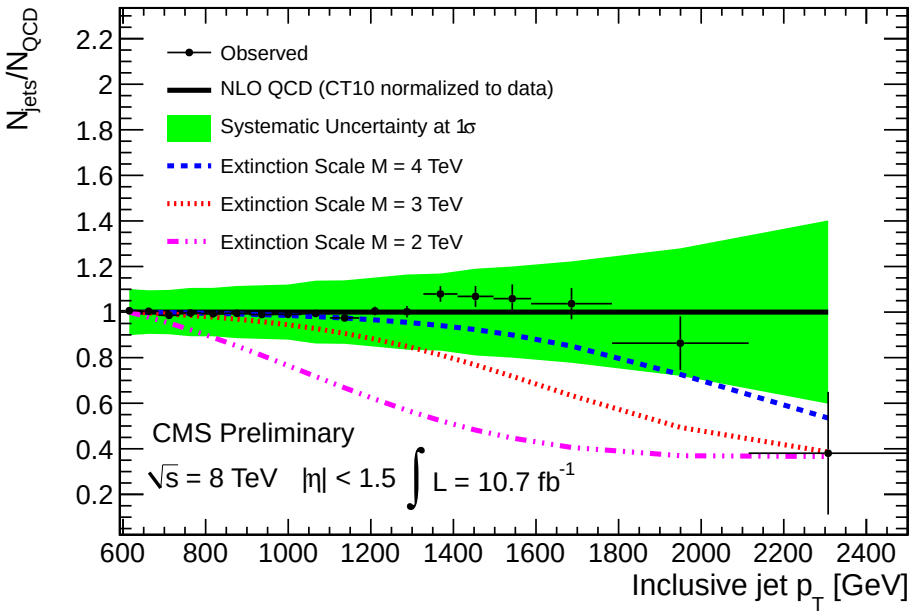

Figure 2: The ratio of the inclusive jet-p_{T} spectrum to the NLO QCD prediction with non-perturbative corrections and convolved with the detector resolution. The colored band shows the magnitude of all sources of systematic uncertainty added in quadrature at 1σ, including JES, JER, PDFs, and luminosity. Dashed lines indicate the effects of extinction at three different values of the extinction scale, $M = 2$, 3, and 4 TeV.

$$\lambda(\mu) = \frac{L(\mu|\hat{\hat{\vec{\theta}}})}{L(\hat{\mu}|\hat{\vec{\theta}})} \tag{3}$$

where the numerator is the maximum of the likelihood function given a signal strength μ, where nuisance parameters take the value $\hat{\hat{\vec{\theta}}}$, and the denominator is the maximum of the likelihood function over the entire parameter space, which occurs for $\mu = \hat{\mu}$ and nuisances $\hat{\vec{\theta}}$. The test statistic Q is then computed by:

$$Q = -2\ln(\lambda(\mu)). \tag{4}$$

The null hypothesis is defined as SM NLO jet production. The extinction hypothesis is defined as the product of the null hypothesis and $F(p_{\mathrm{T}}, M)$ for a given value of β. The variable β is chosen for convenience so that as $\beta \to 0$ the extinction model approaches the SM prediction. In the formal fitting procedure, the value of β is allowed to be negative, and the extinction hypothesis can cross $\beta = 0$ without resulting in a numerical divergence. Negative values of β are modeled by reflecting the extinction function about $F(p_{\mathrm{T}}, M) = 1$. Including systematic uncertainties, the best-fit value of β is (0.008 ± 0.034) TeV $^{-2}$, which is consistent with the SM expectation.

We set limits using the modified frequentist criterion $\mathrm{CL_s}$ [34, 35] with the test statistic described above. All sources of systematic uncertainty are treated as nuisance parameters with log-normal prior constraints and are constructed in the likelihood to have the same value across all jet p_{T} bins. This construction implicitly assumes that the systematic uncertainties are completely correlated in jet p_{T}.

To account for correlations in the JES and PDF uncertainties between p_T bins, we subdivide them into their underlying components. These individual components are strongly correlated across all p_T bins and tend to be dominant at different values of jet-p_T. As an example, uncertainties on the gluon PDF will be dominant at low p_T compared to uncertainties on the quark PDFs. For the JES uncertainty, this means decomposing the uncertainty into each of its orthogonal sources. For the PDF uncertainty, this means evaluating separately the contributions from each of the pairs of eigenvectors in the CT10 [23] PDF set. The search is then repeated with respect to the MSTW2008 [36] PDF set. CT10 predicts the highest inclusive jet cross-section at high p_T among those in wide use, while MSTW2008 is among the lowest. The results derived with respect to these two PDF sets serve as bounds on the result expected when using other sets. This includes the sets which are used in comparison to dedicated measurements of the inclusive jet production cross-section [17], such as NNPDF [37], HERA [38] or ABKM [39].

The CT10 PDF set comprises a central prediction and 26 eigenvector pairs. The central prediction assumes all PDF input parameters are set at their central values. Each eigenvector pair corresponds to the positive and negative uncertainty in one of those input parameters. The difference between the predictions of each eigenvector pair and the central prediction is taken as a source of systematic uncertainty at $\pm 1\sigma$. A source of systematic uncertainty is defined as non-trivial if, at one sigma in either direction, it produces a shift in any p_T bin greater than 1% of the central occupancy. Under this definition, 15 of the 26 CT10 eigenvectors are found to be non-trivial. The relative uncertainty described by the variation between these 15 eigenvector sets and the central prediction is shown in Fig. 3 as a function of jet p_T. The uncertainties associated with the renormalization and factorization scales are computed by varying the scales coherently up and down a factor of 2 and $1/2$, respectively. The nuisance parameters associated with the PDF sets are implemented as p_T-dependent scale factors. As the effect of extinction on the jet-p_T spectrum is expressed relative to the SM prediction, by construction the PDF nuisance parameters have no effect on the signal shape.

Given the exponentially falling nature of the inclusive jet p_T spectrum, uncertainty on the JES is one of the dominant sources of systematic uncertainty. The JES uncertainty is composed of 19 orthogonal sources. Of these, seven are found to be non-trivial according to the criterion defined above: the absolute p_T scale, the single pion response in the ECAL and HCAL, the flavor composition correction, the time dependence, the pileup p_T scale, and the extrapolation of the absolute scale into the high p_T regime [26]. The effects of JER are also included as nuisance parameters. The JES and JER nuisance parameters are implemented as a smearing matrix that specifies the fraction of events that migrate from one jet-p_T bin to another as a function of the strength of the nuisance parameter. The uncertainty in luminosity is taken as a constant scale factor with a 4.4% relative uncertainty [40]. The relative uncertainty of all non-trivial detector-related sources of systematic uncertainty (JES, JER and luminosity) is shown in Fig. 4 as a function of jet p_T.

For each value of the signal strength β, the p-value of the alternative hypothesis p_μ and null hypothesis p_0 are calculated. In a frequentist approach, these p-values are derived by producing an ensemble of pseudoexperiments assuming the null hypothesis, and a separate ensemble assuming the alternative hypothesis. The profile-likelihood test statistic defined above is calculated for each pseudo-experiment, and compared to the value as observed in data. The test statistic is positive definite, with a value of zero corresponding to perfect agreement between the model and the dataset. The p-values represent the fraction of pseudo-experiments with a greater value of the test statistic than the observed one from the data. The statistic CL_s is defined as the ratio $p_\mu/(1-p_0)$. Any value of β for which $CL_s < 0.05$ is regarded as excluded at 95% confidence level (CL). The value of CL_s as a function of β is shown in Fig. 5. The observed

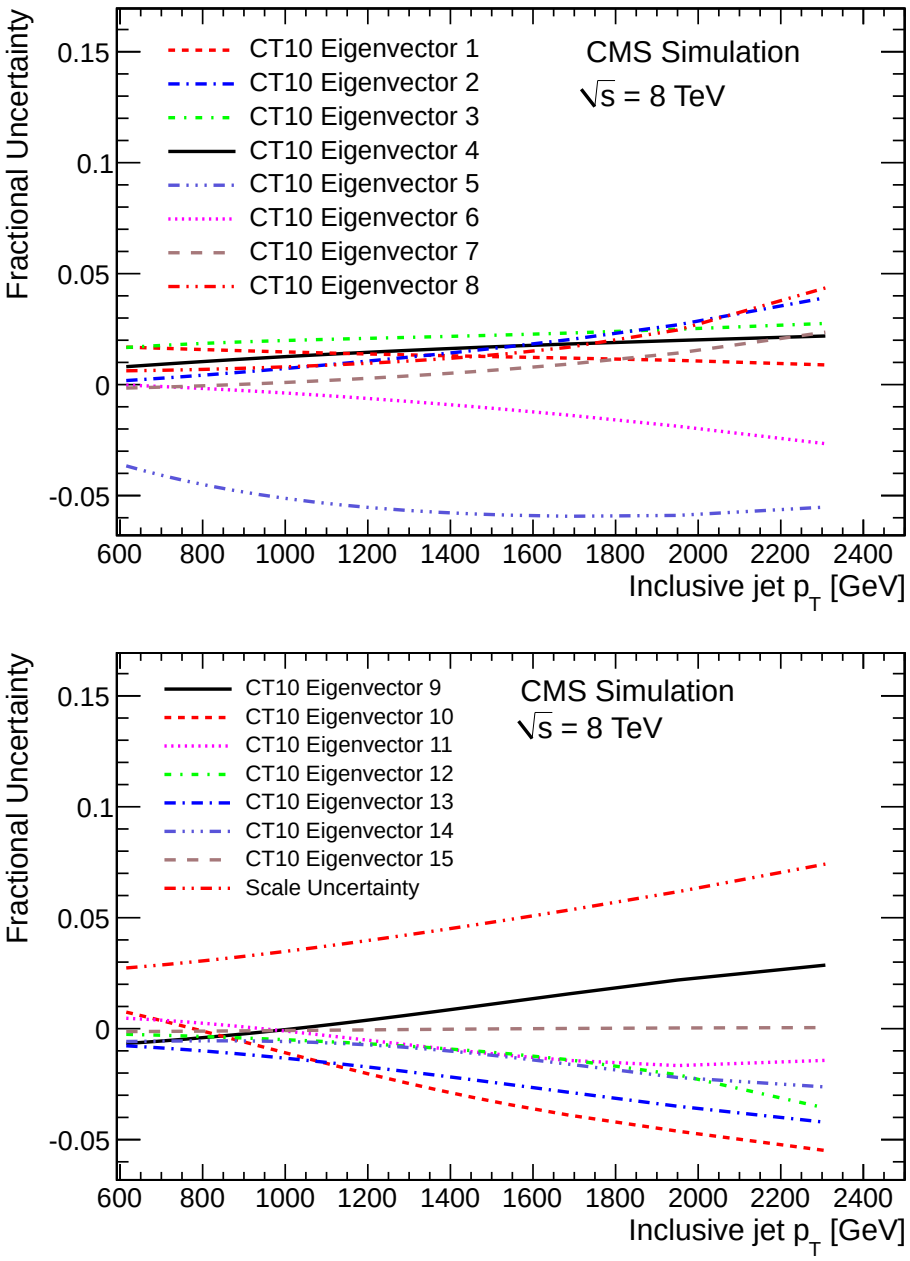

Figure 3: Systematic uncertainty described by systematic variations of the CT10 eigenvectors [23] at 1σ, expressed as a fraction of the central occupancy of each p_{T} bin. Each eigenvector is associated with an uncertainty in a single PDF input parameter. The 15 eigenvectors (out of 26 total) which deviate non-trivially from the central prediction are represented, as is the uncertainty due to variation of the renormalization and factorization scales.

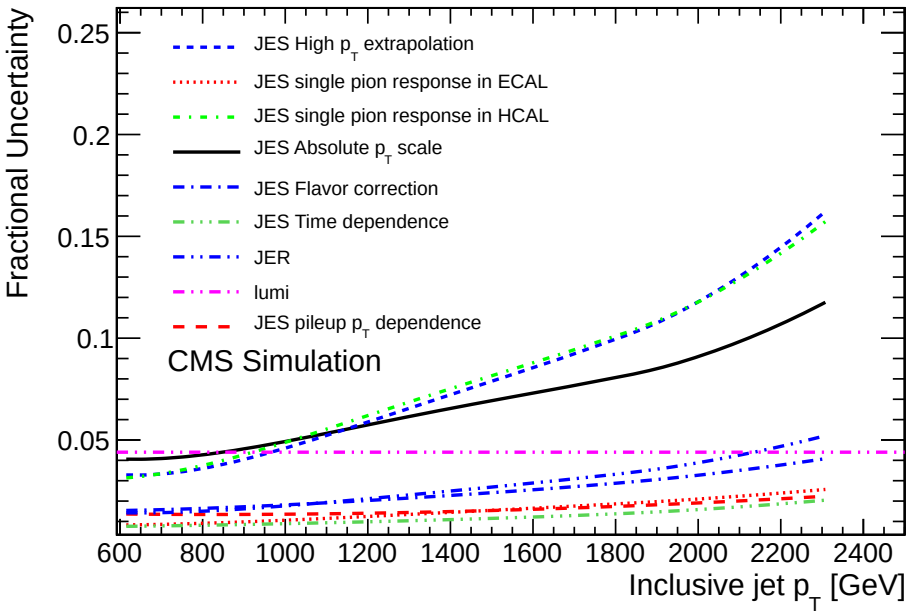

Figure 4: Systematic uncertainty from all experimental sources at 1σ, expressed as a fraction of the central occupancy of each p_{T} bin. The luminosity is a simple scale factor, while the JES and JER uncertainties are modelled as transfer matrices between all p_{T} bins. The seven non-trivial sources of JES uncertainty are shown (out of 19 total).

upper limit on β is 0.091 TeV^{-2} at 95% CL, translating to an observed lower limit on M of 3.3 TeV. The expected upper limit on β is 0.090 TeV^{-2} at 95% CL, corresponding to an expected lower limit on M of 3.4 TeV. These relatively close expected and observed values reflect strong agreement between the observed data and the null hypothesis.

As an additional cross-check, the limit-setting procedure is repeated using the MSTW2008 PDF set [36] as the background hypothesis. The limits given CT10 and MSTW2008 agree to within 10%. MSTW2008 predicts a higher cross-section at very high jet-p_{T} compared to CT10, so the limit produced in this cross-check is predictably less conservative. The predictions of CT10 and MSTW2008 at NLO bound the cross-sections expected by many other commonly-used PDF sets. We can then assume that the results obtained using CT10 and MSTW2008 as our background hypothesis will similarly bound the set of exclusion limits expected if the limit procedure was repeated for all of these sets.

6 Conclusion

In summary, a search for the extinction of jet production has been performed at the LHC in data collected with the CMS detector corresponding to 10.7 fb^{-1} of pp collisions at $\sqrt{s} = 8$ TeV. The extinction model studied in this analysis is motivated by the search for signatures of terascale gravity at the LHC and assumes the existence of string couplings in the strong-coupling limit. In this limit, the string model predicts suppression of high-p_{T} jet production beyond an extinction scale M. A detailed comparison between the measured p_{T} spectrum and the theoretical prediction is conducted. No significant deficit of events is found at high transverse momentum. A 95% CL lower limit of 3.3 TeV is set on the extinction parameter M.

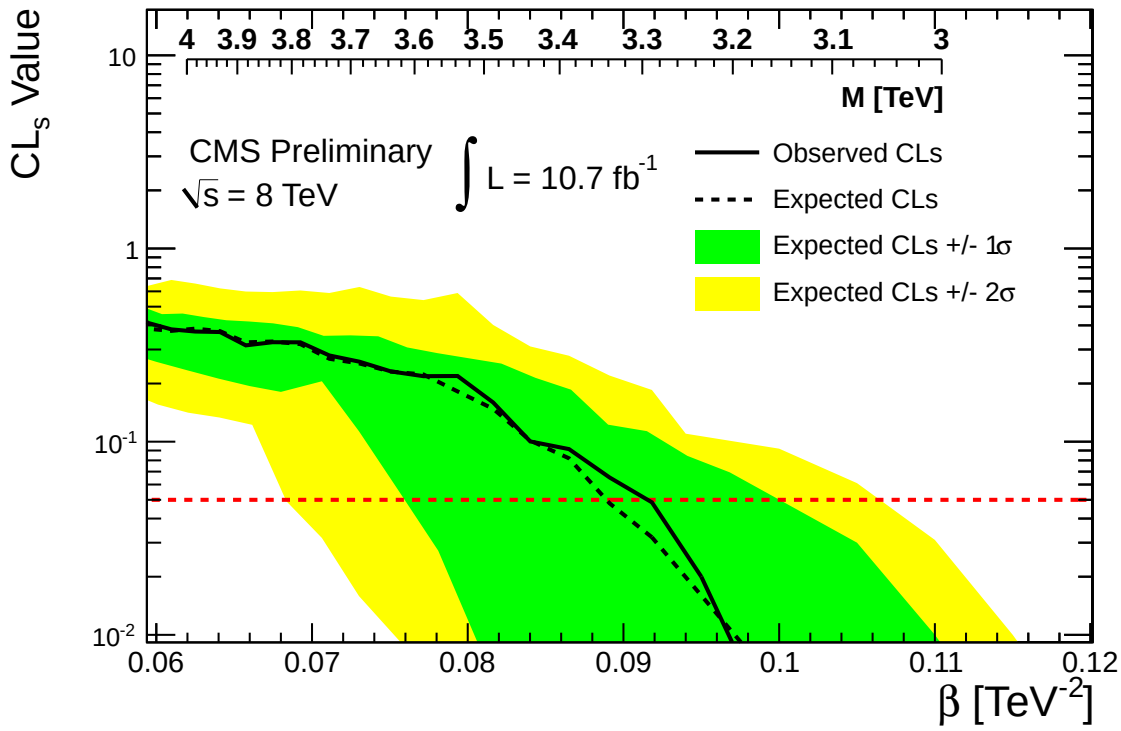

Figure 5: The results of a CL_s scan in the extinction scale, $\beta = M^{-2}$. The observed value of CL_s as a function of β is shown by the solid line. The observed upper limit on β is 0.091 TeV^{-2} at 95% confidence level (CL), corresponding to a lower limit of 3.3 TeV on the extinction scale M. The dashed line indicates the expected median of results for the background-only hypothesis. The green (dark) and yellow (light) bands indicate the ranges that are expected to contain 68% and 95% of all observed excursions of the background from the median, respectively.

References

[1] T. Banks and W. Fischler, "A Model for High Energy Scattering in Quantum Gravity", (1999). arXiv:hep-th/9906038.

[2] CMS Collaboration, "Search for microscopic black holes in pp collisions at $\sqrt{(s)}$ = 7 TeV", *JHEP* **04** (2012) 061, doi:10.1007/JHEP04(2012)061.

[3] CMS Collaboration, "Search for Signatures of Extra Dimensions in the Diphoton Mass Spectrum at the Large Hadron Collider", *Phys. Rev. Lett.* **108** (2012) 111801, doi:10.1103/PhysRevLett.108.111801.

[4] CMS Collaboration, "Search for Resonances in the Dijet Mass Spectrum from 7 TeV pp Collisions at CMS", *Phys. Lett. B* **704** (2011) 123, doi:10.1016/j.physletb.2011.09.015.

[5] CMS Collaboration, "Search for Resonances in the Dilepton Mass Distribution in pp Collisions at $\sqrt{(s)} = 7$ TeV", *JHEP* **05** (2011) 093, doi:10.1007/JHEP05(2011)093.

[6] ATLAS Collaboration, "Search for strong gravity signatures in same-sign dimuon final states using the ATLAS detector at the LHC", *Phys. Lett. B* **709** (2012) 322, doi:10.1016/j.physletb.2012.02.049.

[7] ATLAS Collaboration, "Search for Extra Dimensions using diphoton events in 7 TeV proton-proton collisions with the ATLAS detector", *Phys. Lett. B* **710** (2012) 538, doi:10.1016/j.physletb.2012.03.022.

[8] ATLAS Collaboration, "Search for new particles decaying to ZZ using final states with leptons and jets with the ATLAS detector in $\sqrt{s}$ = 7 Tev proton-proton collisions", *Phys. Lett. B* **712** (2012) 331, doi:10.1016/j.physletb.2012.05.020.

[9] CMS Collaboration, "Search for dark matter and large extra dimensions in monojet events in pp collisions at sqrt(s)= 7 TeV", (2012). arXiv:1206.5663. Submitted to JHEP.

[10] CMS Collaboration, "Search for Dark Matter and Large Extra Dimensions in pp Collisions Yielding a Photon and Missing Transverse Energy", *Phys. Rev. Lett.* **108** (2012) 261803, doi:10.1103/PhysRevLett.108.261803.

[11] L. Randall and R. Sundrum, "A large mass hierarchy from a small extra dimension", *Phys. Rev. Lett.* **83** (1999) 3370, doi:10.1103/PhysRevLett.83.3370.

[12] N. Arkani-Hamed, S. Dimopoulos, and G. Dvali, "Phenomenology, astrophysics and cosmology of theories with submillimeter dimensions and TeV scale quantum gravity", *Phys. Rev. D* **59** (1999) 086004, doi:10.1103/PhysRevD.59.086004.

[13] S. B. Giddings and S. D. Thomas, "High energy colliders as black hole factories: The end of short distance physics", *Phys. Rev. D* **65** (2002) 056010, doi:10.1103/PhysRevD.65.056010.

[14] G. Landsberg and S. Dimopoulos, "Black Holes at the LHC", *Phys. Rev. Lett.* **87** (2001) 161602, doi:10.1103/PhysRevLett.87.161602.

[15] P. Meade and L. Randall, "Black Holes and Quantum Gravity at the LHC", *JHEP* **05** (2008) 003, doi:10.1088/1126-6708/2008/05/003.

[16] C. Kilic et al., "Jet Extinction from Non-Perturbative Quantum Gravity Effects", (2012). arXiv:1207.3525. Submitted to PRD.

[17] CMS Collaboration, "Measurement of the Inclusive Jet Cross Section in pp Collisions at sqrt(s) = 7 TeV", *Phys. Rev. Lett.* **107** (2011) 132001, doi:10.1103/PhysRevLett.107.132001.

[18] CMS Collaboration, "The CMS experiment at the CERN LHC", *JINST* **3** (2008) S08004, doi:10.1088/1748-0221/3/08/S08004.

[19] "The CMS high level trigger", *Eur. Phys. J. C* **46** (2006) 605, doi:10.1140/epjc/s2006-02495-8.

[20] Z. Nagy, "Three-jet cross sections in hadron hadron collisions at next-to-leading order", *Phys. Rev. Lett.* **88** (2002) 122003, doi:10.1103/PhysRevLett.88.122003.

[21] Z. Nagy, "Next-to-leading order calculation of three-jet observables in hadron-hadron collision", *Phys. Rev. D* **68** (2003) 094002, doi:10.1103/PhysRevD.68.094002.

[22] T. Kluge, K. Rabbertz, and M. Wobisch, "Fast pQCD calculations for PDF fits", in *14th International Workshop on Deep Inelastic Scattering (DIS 2006), 20-24 Apr 2006*, p. 483. Tsukuba, Japan, April, 2006. doi:10.1142/9789812706706_0110.

[23] P. M. Nadolsky et al., "Implications of CTEQ global analysis for collider observables", *Phys. Rev. D* **78** (2008) 013004, doi:10.1103/PhysRevD.78.013004.

[24] T. Sjöstrand, S. Mrenna, and P. Z. Skands, "PYTHIA 6.4 Physics and Manual", *JHEP* **05** (2006) 026, doi:10.1088/1126-6708/2006/05/026.

[25] M. Bähr et al., "Herwig++ physics and manual", *European Physical Journal C* **58** (2008) 639–707, arXiv:0803.0883.

[26] CMS Collaboration, "Determination of the Jet Energy Scale in CMS with pp Collisions at $\sqrt{s} = 7$ TeV", CMS Physics Analysis Summary CMS-PAS-JME-10-010, (2010).

[27] E. A. Mirabelli, M. Perelstein, and M. E. Peskin, "Collider signatures of new large space dimensions", *Phys. Rev. Lett.* **82** (1999) 2236–2239, doi:10.1103/PhysRevLett.82.2236.

[28] D. Lust, S. Stieberger, and T. R. Taylor, "The LHC String Hunter's Companion", *Nucl. Phys. B* **808** (2009) 1, doi:10.1016/j.nuclphysb.2008.09.012.

[29] CMS Collaboration, "Commissioning of the Particle-flow Event Reconstruction with the First LHC Collisions Recorded in the CMS Detector", CMS Physics Analysis Summary CMS-PAS-PFT-10-001, (2010).

[30] M. Cacciari, G. P. Salam, and G. Soyez, "The anti-k_t jet clustering algorithm", *JHEP* **04** (2008) 063, doi:10.1088/1126-6708/2008/04/063.

[31] CMS Collaboration, "Identification and filtering of uncharacteristic noise in the CMS hadron calorimeter", *Journal of Instrumentation* **5** (2010) 3014, doi:10.1088/1748-0221/5/03/T03014, arXiv:0911.4881.

[32] CMS Collaboration, "Calorimeter Jet Quality Criteria for the First CMS Collision Data", CMS Physics Analysis Summary CMS-PAS-JME-09-008, (2010).

[33] G. Cowan et al., "Asymptotic formulae for likelihood-based tests of new physics", *European Physical Journal C* **71** (2011) 1554, doi:10.1140/epjc/s10052-011-1554-0.

[34] T. Junk, "Confidence level computation for combining searches with small statistics", *Nucl. Instrum. Meth. A* **434** (1999) 435, doi:10.1016/S0168-9002(99)00498-2.

[35] A. L. Read, "Presentation of search results: The CL(s) technique", *J. Phys. G* **28** (2002) 2693, doi:10.1088/0954-3899/28/10/313.

[36] A. D. Martin et al., "Parton distributions for the LHC", *Eur. Phys. J. C* **63** (2009) 189, doi:10.1140/epjc/s10052-009-1072-5.

[37] R. D. Ball et al., "A first unbiased global NLO determination of parton distributions and their uncertainties", *Nuclear Physics B* **838** (2010) 136–206, doi:10.1016/j.nuclphysb.2010.05.008.

[38] F. D. Aaron et al., "Combined measurement and QCD analysis of the inclusive e p scattering cross sections at HERA", *Journal of High Energy Physics* **1** (2010) 109, doi:10.1007/JHEP01(2010)109.

[39] S. Alekhin et al., "3-, 4-, and 5-flavor next-to-next-to-leading order parton distribution functions from deep-inelastic-scattering data and at hadron colliders", *Phys. Rev. D* **81** (2010) 014032, doi:10.1103/PhysRevD.81.014032.

[40] CMS Collaboration, "Absolute Calibration of the Luminosity Measurement at CMS: Winter 2012 Update", CMS Physics Analysis Summary CMS-PAS-SMP-12-008, (2012).